Simulations of water transport through carbon nanotubes: How different water models influence the conduction rate

L. Liu and G. N. Patey

Citation: The Journal of Chemical Physics **141**, 18C518 (2014); doi: 10.1063/1.4896689
View online: http://dx.doi.org/10.1063/1.4896689
View Table of Contents: http://scitation.aip.org/content/aip/journal/jcp/141/18?ver=pdfcov
Published by the AIP Publishing

Simulations of water transport through carbon nanotubes: How different water models influence the conduction rate

L. Liu and G. N. Patey[a)]
Department of Chemistry, University of British Columbia, Vancouver, British Columbia V6T 1Z1, Canada

(Received 12 July 2014; accepted 17 September 2014; published online 2 October 2014)

The conduction rate of water through (8,8) and (9,9) carbon nanotubes at 300 K and a pressure difference of 220 MPa is investigated using molecular dynamics simulations. The TIP3P, SPC/E, and TIP4P/2005 water models are considered. The pressure-driven flow rate is found to be strongly model dependent for both nanotubes. The fastest model (TIP3P) has a flow rate that is approximately five times faster than the slowest (TIP4P/2005). It is shown that the flow rate is significantly influenced by the structure taken on by the water molecules confined in the nanotube channels. The slower models, TIP4P/2005 and SPC/E, tend to favor stacked ring arrangements, with the molecules of a ring moving together through the nanotube, in what we term a "cluster-by-cluster" conduction mode. Confined TIP3P water has a much weaker tendency to form ring structures, and those that do form are fragile and break apart under flow conditions. This creates a much faster "diffusive" conduction mode where the water molecules mainly move through the tube as individual particles, rather than as components of a larger cluster. Our results demonstrate that water models developed to describe the properties of bulk water can behave very differently in confined situations. © *2014 AIP Publishing LLC*. [http://dx.doi.org/10.1063/1.4896689]

I. INTRODUCTION

Understanding mass transport through nanoscale channels is of much current interest, ranging in relevance from biological channels to the search for efficient nano-filtration membranes. In particular, the flow of water and interesting solutes such as ions through carbon nanotubes (CNTs) has received a great deal of attention, and is the focus of an ongoing, substantial research effort.[1–3] Recent experiments[4–6] have reported high water conductance rates through CNTs, and computer simulations have been widely employed in an effort to understand water conduction through CNTs, as well as solute conduction and nanotube selectivity.[7–29]

During the past decade, there have been many investigations of the characteristics of CNTs, including possible modifications, that could influence water and/or solute conduction. For example, channel size,[18,27] charge modification,[22] chemical modification,[19] and nanotube defects[25] have been considered. However, we note that in most simulation studies a particular water model, such as TIP3P,[10–24,30] SPC/E,[7–9,31] TIP5P,[26–28,32] etc., has been adopted, but there has been little discussion of how different water models might influence flow rates. Some authors have considered more than one water model, and have noted some similarities and differences,[29] but there appears to have been no systematic study of different models under pressure-driven, non-equilibrium conditions.

There have been a few systematic model comparisons employing equilibrium molecular dynamics (MD) simulations. Recently, Nakamura and Ohno[33] investigated the structure of water in (8,8) and (9,9) CNTs, and their work is particularly interesting because they found substantial structural differences when they compared the TIP3P, TIP4P, and TIP5P-E[34] forcefields. TIP3P water was less ordered than the other two models, which tended to form stacked ring structures. Alexiadis and Kassinos[35,36] examined density, hydrogen bonding, and self-diffusivity of water confined in CNTs of various diameters, and reached a similar conclusion concerning the relative lack of order displayed by TIP3P. This is also consistent with the results of Bauer *et al.*[37] who considered different water models confined between hydrophobic surfaces.

However, as noted above, all of these model comparisons apply to equilibrium conditions, and not to pressure-driven flow. Therefore, in the present paper we investigate the behavior of three water models undergoing pressure-driven flow under identical conditions. The models considered are TIP3P, SPC/E, and TIP4P/2005.[38] We selected the TIP3P and SPC/E models because they are among the most popular water models, and included TIP4P/2005 because it gives a very good description of ambient bulk water.[39] We consider both (8,8) and (9,9) CNTs, and find substantially different flow rates for the different models. At a pressure differences of 220 MPa, the flow rate for TIP3P is approximately five times higher than that of TIP4P/2005, with SPC/E lying between the two, but closer to TIP4P/2005. We trace the different flow rates to the different structure of the confined water, and show that depending on the amount and nature of the structure, one can have different modes of water conduction.

It is important to emphasize that the results reported here are applicable to (8,8) and (9,9) nanotubes which are wide enough to accommodate water structures such as four-, five-, and six-membered rings. In narrower nanotubes [e.g., (6,6)] such structures do not occur and water molecules in the nanotube channel form only hydrogen-bonded chains.[10–17]

a)patey@chem.ubc.ca

We would not expect the single-file conduction mode[10,12] observed for such nanotudes to be very sensitive to the water model employed because the differing tendencies of water models to form ring structures is not a factor in nanotubes which are too narrow for such structures to occur.

The remainder of this paper is divided into three parts. The model and simulation method are described in Sec. II, the results in Sec. III, and our conclusions are summarized in Sec. IV.

II. MODELS AND METHODS

The simulation setup is illustrated in Fig. 1. Parallel graphene sheets located in the *xy* plane are used to divide the simulation cell into two regions connected by a carbon nanotube, with its symmetry axis parallel to *z*. Appropriate openings are made in the graphene sheet allowing water to pass through the nanotube joining the two regions of the simulation cell. The graphene sheets together with the nanotube can be viewed as a part of a water permeable membrane. The membrane is rigid with the positions of all carbon atoms held fixed during the simulation. In this paper, we consider (8,8) and (9,9) armchair CNTs. To estimate the water density, the volume of the water bearing region of the cell, including the nanotube, is calculated assuming that a carbon atom has a van der Waals radius of 0.17 nm. This gives effective internal diameters of 0.75 nm and 0.88 nm for the (8,8) and (9,9) CNTs, respectively. In all simulations the nanotube length was fixed at 3.561 nm, and unless otherwise stated the (*x*, *y*, *z*) cell dimensions were (5.116 nm, 5.168 nm, 7.569 nm). The density of water was fixed at 1 g/ml, such that the simulations included 3299 and 3322 water molecules for the (8,8) and (9,9) CNTs, respectively.

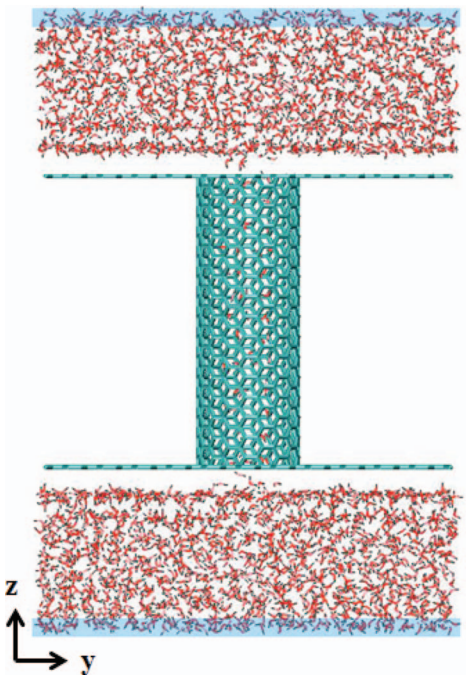

FIG. 1. Diagram of the simulation cell. Carbon atoms are cyan, oxygen atoms are red, and hydrogen atoms are gray. The blue shading denotes the regions where the external force is applied. The (*x*, *y*, *z*) cell dimensions are (5.116 nm, 5.168 nm, 7.569 nm), the nanotube is 3.561 nm long.

TABLE I. Forcefield parameters used in the simulations. σ is in Å, ε is in kJ/mol, and charges are in units of *e*.

Water model	σ_O	ε_O	q_H	q_O	q_M
TIP4P/2005	3.1589	0.7749	+0.5564	0	−1.1128
SPC/E	3.1658	0.6502	+0.4238	−0.8476	0
TIP3P	3.1506	0.6364	+0.4170	−0.8340	0
Carbon model	σ_C	ε_C		q_C	
AMBER03	3.3997	0.3598		0	

In our simulations a pressure difference across the membrane is created by applying an appropriate force in the *z* direction to a layer of water molecules, ideally located far from the membrane (see below). To ensure that our results are not unduly sensitive to this distance, some simulations were carried out at essentially double the *z* dimension of the bulk water region, requiring in excess of 6000 water molecules. As discussed below, these simulations revealed no significant qualitative dependence of conduction rates on the size of the bulk region.

We consider three commonly used water models: TIP4P/2005,[38] SPC/E,[31] and TIP3P.[30] We are particularly interested in the TIP4P/2005 model because of its excellent descriptions of overall water properties.[39] In our model systems all site-site interactions consist of Lennard-Jones (LJ) and/or Coulombic terms. The interaction parameters for all three water models as well as for carbon atoms are summarized in Table I. The parameters for a carbon atom are adopted from the AMBER03 forcefield.[40] The Lorentz-Berthelot combining rules are used to calculate the Lennard-Jones interactions.

All MD simulations were carried out using the GROMACS 4.5.5 package.[41] Three dimensional periodic boundary conditions (PBC) were applied, and the particle mesh Ewald algorithm[42] was used to compute electrostatic interactions. The temperature was controlled at 300 K employing a refined velocity rescaling algorithm.[43] A time step of 1 fs was used in the simulations, which were typically performed for 10 ns. Approximately 1 ns was required to achieve steady state flow, and data for analysis were collected over the remaining 9 ns. For each CNT/water model combination considered, five "replica" simulations with different initial conditions were performed in order to estimate statistical uncertainties. The results presented below are averages of the five replica results.

In order to create a pressure difference, Δp, across the membrane we use the method proposed by Zhu *et al.*[44] In this method, a constant force in the *z* direction is applied to a subset of water molecules located at the top and bottom of the periodic simulation cell (see Fig. 1). This corresponds to a pressure difference of

$$\Delta p = \frac{nf}{A}, \tag{1}$$

where *n* is the total number of molecules in the subset, *f* is the constant force, and *A* is the area of membrane. In our simulations the subset of molecules experiencing the force

were located in two layers each 0.2 nm thick, as shown in Fig. 1. On average this subset included ∼360 water molecules. Note that the force is applied only to the oxygen atoms of the water molecules to avoid instigating additional molecular rotation. In order to efficiently implement this algorithm on the GROMACS platform, the subset list was updated every 10 ps, rather than at every time step. However, this does not influence the observed flow rates, which were the same for update times of 5 or 25 ps. We also verified that within reason varying the thickness of the layers (e.g., increasing to 0.4 nm) over which the force is applied has no significant qualitative effect, which, as noted above, is also true of the amount of bulk water included in the cell. All results reported in this paper are for a pressure difference of 220 MPa.

III. RESULTS AND DISCUSSION

The flow rate, defined as the number of molecules that pass through the nanotube (enter one end and exit the other) per unit time, is often used to describe and compare the conduction behavior of CNTs.[7,22] Cumulative counts of water molecules passing through the nanotubes as functions of time for typical simulations are shown in Fig. 2. Note that there are six systems in total, consisting of all combinations of three water models and two CNTs of different size. From Fig. 2 we see that the counts are essentially linear in time indicating that steady state flow has been established. In all systems, we observe only unidirectional flow as expected for a pressure difference as high as 220 MPa. It is also obvious from Fig. 2 that the flow rates are not the same for the different water models.

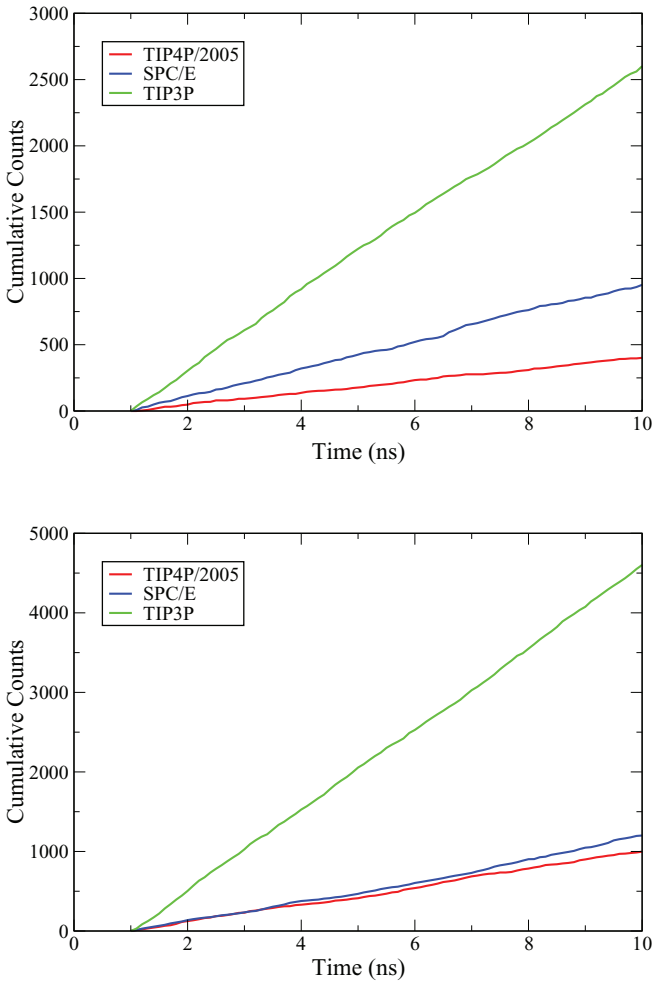

FIG. 2. Cumulative curves showing the number of water molecules that have passed through (8,8) (top panel) and (9,9) (bottom panel) nanotubes as functions of time. The red, blue, and green curves are for the TIP4P/2005, SPC/E, and TIP3P models, respectively.

Average flow rates together with standard deviations estimated using five independent simulations each of 10 ns are given in Table II. The flow rates obtained for larger systems containing more bulk water as described above are also included. Only two simulations of 5 ns each were carried out for the larger systems, so no error estimates were obtained. Nevertheless, for all six systems we note that the larger system values are close to those of the smaller system, particularly considering the error estimates for the smaller system. The results given in Table II demonstrate that for identical conditions the flow rates can strongly depend on the water model employed. The TIP3P model has the highest flow rate, TIP4P/2005 water is slower by approximately a factor of five, and SPC/E lies in between but is also much slower than TIP3P.

So, why do different water models exhibit such different flow rates? To address this question, we examine the structure of water confined within the nanotubes. Based on examination of different configurations for different water models, it proved instructive to classify confined water molecules as being in one of two potential states. We label one state "ring-bound" indicating that the molecule forms a ring configuration together with other adjacent molecules. Ring configurations are defined as collections of four, five, or six water molecules arranged such that to within some specified width, their oxygen atoms lie in a plane orthogonal to the symmetry axis of the nanotube. In our analysis, molecules are considered to be part of the same ring configuration if the differences in the axial coordinates of their oxygen atoms are all less than 0.15 nm. We find that this condition is sufficient to identify ring structures that are essentially planar. Because of spatial constraint, four member rings (square configurations) are dominant within the (8,8) nanotube, whereas five (pentagons) and six (hexagons) member rings can be found in the larger (9,9) nanotube. As an example, a four member square ring is

TABLE II. Selected properties for different water models in the (8,8) and (9,9) nanotubes. "Flow rate" is the average number of water molecules passing through the nanotube channel during a period of 1 ns. The rightmost numbers in the "Flow rate" column are the values obtained with the larger system containing approximately twice as much bulk water, as described in the text. The numbers in parenthesis are estimated standard deviations. "Hydrogen bonds" indicates the average number of hydrogen bonds per water molecule located within the nanotube.

	(8,8) nanotube		(9,9) nanotube	
Water model	Flow rate	Hydrogen bonds	Flow rate	Hydrogen bonds
TIP4P/2005	51 (4); 48	3.28	107 (6); 116	3.22
SPC/E	111 (4); 120	3.02	134 (14); 152	3.28
TIP3P	287 (5); 287	2.66	492 (15); 502	2.75

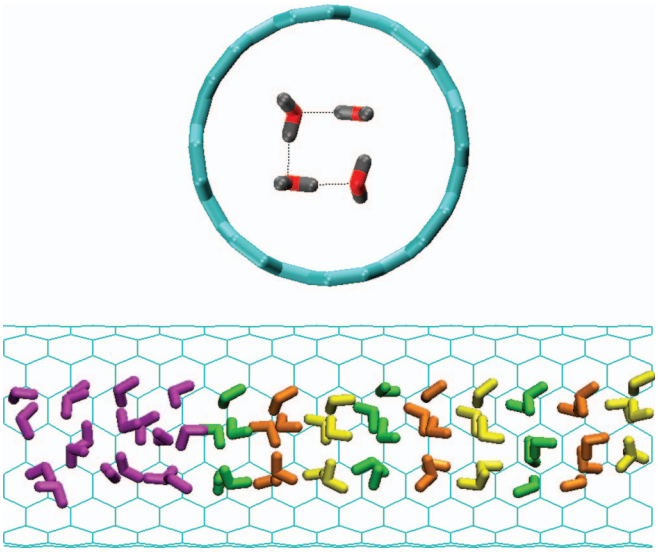

FIG. 3. (Top panel) A square ring of water molecules in the (8,8) nanotube. Carbon atoms are cyan, oxygen atoms are red, and hydrogen atoms are gray. The black dotted lines indicate hydrogen bonds. (Bottom panel) A configurational snapshot of TIP4P/2005 water in the (9,9) nanotube. Ring-free water molecules are magenta, and stacked ring structures are repeating green, orange and yellow. Note that part of carbon nanotube is not displayed for clarity.

illustrated in Fig. 3 (top panel). All confined water molecules that are not identified as being part of a ring are labeled as "ring-free." A configurational snapshot of TIP4P/2005 water in a (9,9) nanotube is shown in Fig. 3 (bottom panel). The ring-bound molecules are indicated with a repeating green, orange, and yellow color scheme, with molecules of the same color forming particular pentagonal ring configurations. The ring-free molecules are colored magenta, and these appear as more randomly positioned and oriented. Note that molecules can and do switch between ring-bound and ring-free states as the simulation progresses.

It is interesting to note that the ring clusters stacked along the axial direction of the nanotube [Fig. 3 (bottom panel)] somewhat resemble the ice structures reported in CNTs at lower temperatures.[45] However, in the present case ring-free molecules also exist in the nanotube, and there is no long-range order as in ice. We shall see below that it is the relative prevalence of ring structures that influences the conduction properties of the different water models.

In order to gain insight into how the structure of water in a nanotube influences the flow rate, we analyze all systems considered in terms of ring-bound and ring-free molecules. Further, we divide the ring-bound molecules into those that are part of square, pentagonal, and hexagonal rings. The results are summarized for (8,8) and (9,9) nanotubes in Tables III and IV, respectively. Due to spatial constraint, there are very few pentagons, and no hexagons found in the (8,8) nanotube (Table III), whereas, all three ring structures can and do exist in the (9,9) case. It is obvious from Tables III and IV that the average fractions of ring-bound and ring-free molecules vary substantially for the different models. For the (8,8) nanotude TIP4P/2005 has the fewest ring-free molecules (3.1%), and TIP3P the most (71.0%), with SPC/E lying in between (25.2%). It is interesting to note that the structural differences we see amongst the different models under flow are qualitatively similar to those found by Nakamura and Ohno[33] under equilibrium conditions, although these authors considered the original TIP4P model,[30] rather than TIP4P/2005.

TABLE III. Percentage of water molecules in different structural states in the (8,8) nanotube.

Water model	Squares (%)	Pentagons (%)	Hexagons	Ring-free (%)
TIP4P/2005	96.7	0.2	0	3.1
SPC/E	74.2	0.6	0	25.2
TIP3P	28.7	0.3	0	71.0

Comparing Tables II and III, there is clearly a direct correlation between the flow rate and the fraction of ring-free molecules, with TIP3P having the largest fraction of ring-free molecules and the highest flow rate. The situation is similar for the (9,9) nanotube, where again TIP3P has the largest fraction of ring-free molecules (Table IV), and the fastest rate of flow (Table II). TIP4P/2005 and SPC/E have the same ring-free fraction (12.6%) for the (9,9) case, and we see from Table II that the flow rates for these models are similar, with the SPC/E rate a little higher than that of TIP4P/2005. We do note that although the fraction of ring-bound molecules is the same for TIP4P/2005 and SPC/E, the distributions over squares, pentagons, and hexagons differ significantly indicating differences in the structure of the confined water. However, these differences appear to have only a small, if any, effect on the flow rates.

Significant model differences are also apparent in probability distribution functions, $P(N_{nt})$, for the number of water molecules, N_{nt}, confined within the nanotubes, as shown in Fig. 4. Considering first the (8,8) nanotube [Fig. 4 (top panel)], we note that for the SPC/E and TIP3P models the $P(N_{nt})$ distributions are unimodal, whereas the TIP4P/2005 distribution is bimodal, with quite sharp peaks at 48 and 52 molecules. The fact that for TIP4P/2005 96.7% of the water molecules in the nanotube channel occur in square ring configurations (Table III) suggests that these peaks correspond to 12 and 13 square rings, respectively, stacked into the nanotube cavity. For the (9,9) case [Fig. 4 (bottom panel)] TIP3P has fewer ring-bound molecules (Table IV) and on average the fewest molecules in the nanotube. SPC/E has the largest fraction of hexagonal rings (72.3%), and the most molecules in the nanotube cavity; the peak at 72 molecules likely corresponds to configurations where the cavity is filled by 12 hexagonal rings. The TIP4P/2005 model contains significant numbers of both pentagonal (49.2%) and hexagonal (34.9%) rings, as well as ring-free molecules (12.6%). As a result, the

TABLE IV. Percentage of water molecules in different structural states in the (9,9) nanotube.

Water model	Squares (%)	Pentagons (%)	Hexagons (%)	Ring-free (%)
TIP4P/2005	3.3	49.2	34.9	12.6
SPC/E	2.8	12.3	72.3	12.6
TIP3P	12.9	20.0	3.0	64.1

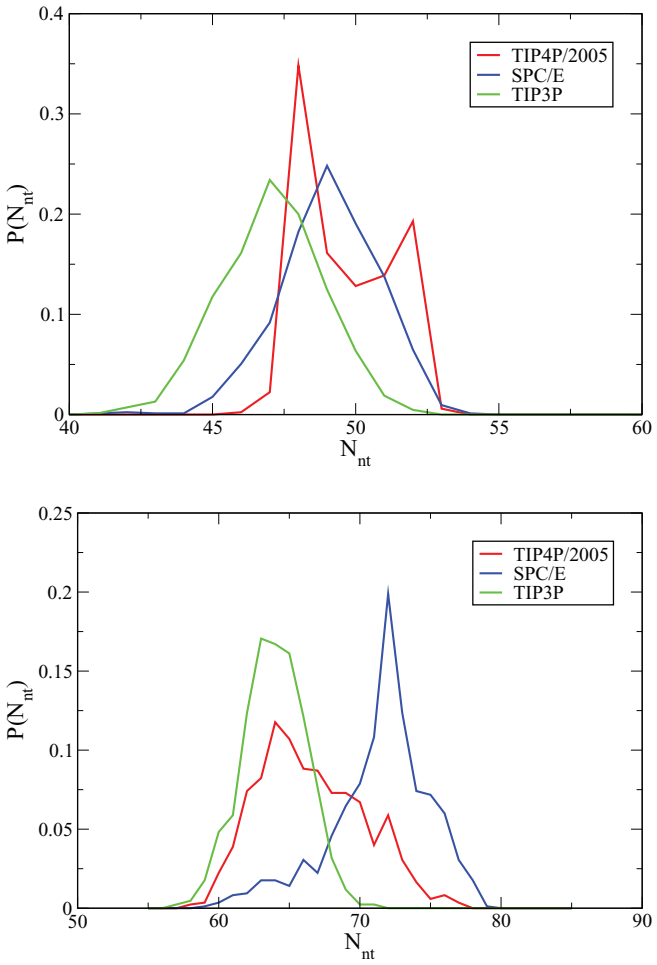

FIG. 4. Probability distributions for the number of confined water molecules in (8,8) (top panel) and (9,9) (bottom panel) nanotubes. The red, blue, and green curves are for the TIP4P/2005, SPC/E, and TIP3P models, respectively.

$P(N_{nt})$ for TIP4P/2005 is quite broad with a main peak at 64 molecules, corresponding to mixed structures, and a more minor peak at 72 molecules which we again associate with 12 hexagonal rings.

In view of the different structures observed for the different models, it is interesting to look at the average number of hydrogen bonds formed by water molecules within the nanotube cavity. If stacked ring structures are favored we would expect both intra-layer hydrogen bonds lying in the plane of the ring, and inter-layer hydrogen bonds joining the rings, generally parallel to the symmetry axis of the nanotube. For more loosely packed structures, we would expect on average fewer hydrogen bonds per molecule. We calculated the average number of hydrogen bonds for water molecules within nanotubes adopting the geometric criteria of Luzar and Chandler.[46] The results are included in Table II, and are in accord with our expectations. In both CNTs, TIP3P water has the fewest hydrogen bonds per molecule, consistent with its having the largest fraction of ring-free molecules. For the (8,8) case, SPC/E has fewer hydrogen bonds than TIP4P/2005, again consistent with its having a larger fraction of ring-free molecules.

Returning to water conduction, we can now understand the different flow rates observed for different models. From

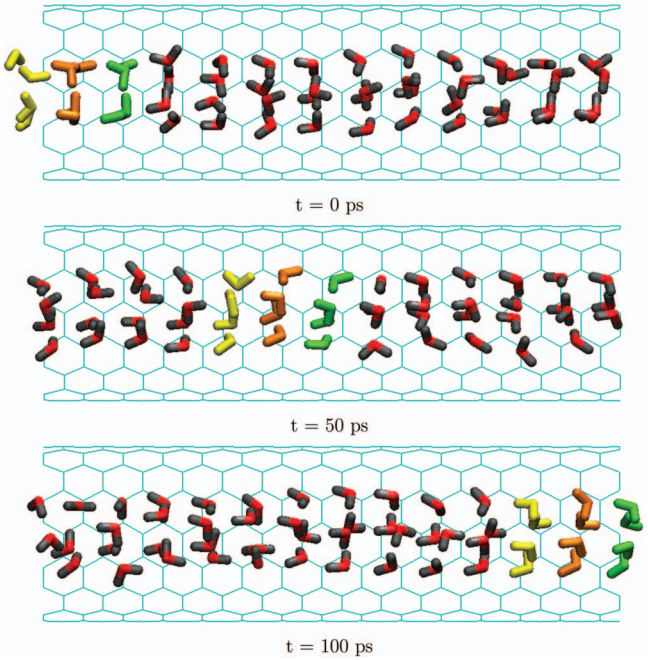

FIG. 5. An illustration of the "cluster-by-cluster" conduction mode for TIP4P/2005 in the (8,8) nanotube. Carbon atoms are cyan, oxygen atoms are red, and hydrogen atoms are gray, except for three square ring configurations highlighted in yellow, orange, and green. We note that the highlighted ring structures pass intact through the nanotube. Note that part of carbon nanotube is not displayed for clarity.

the results given in Tables II–IV, higher flow rates are clearly associated with higher fractions of ring-free molecules. In fact, by closely observing flow through the nanotubes, two conduction modes can be identified. One mode, which we label "cluster-by-cluster," is best represented by TIP4P/2005. In this mode the water molecules assemble into small clusters (rings of some type), that move together through the nanotube, one cluster following the next. For example, for TIP4P/2005 water in the (8,8) nanotube, the clusters are the four-membered rings discussed above. The cluster-by-cluster mode is illustrated in the configurational snapshots shown in Fig. 5. Note that in this particular example the highlighted rings present at $t = 0$, remain intact as they pass through the entire nanotube. This is not always the case and sometimes clusters do break apart, but the conduction involves a significant amount of cluster motion. A second conduction mode, which we label "diffusive," is the main mode of conduction for the TIP3P model. In this case, there are fewer ring structures (Tables III and IV), and those that do occur are fragile and tend to break up during transport. Therefore, the water molecules move through the nanotube more independently, rather than as part of a cluster or group. This is illustrated in Fig. 6, where snapshots are shown for the TIP3P model in the (8,8) nanotube. Note that the apparently square ring structures present at $t = 0$, completely break apart as they flow through the nanotube, and one does not see the cluster-by-cluster flow observed for TIP4P/2005.

Based on this analysis, we conclude that the formation of relatively stable stacked ring structures by the TIP4P/2005 and SPC/E models results in flow rates that are much slower than those observed for TIP3P water. Of course, both

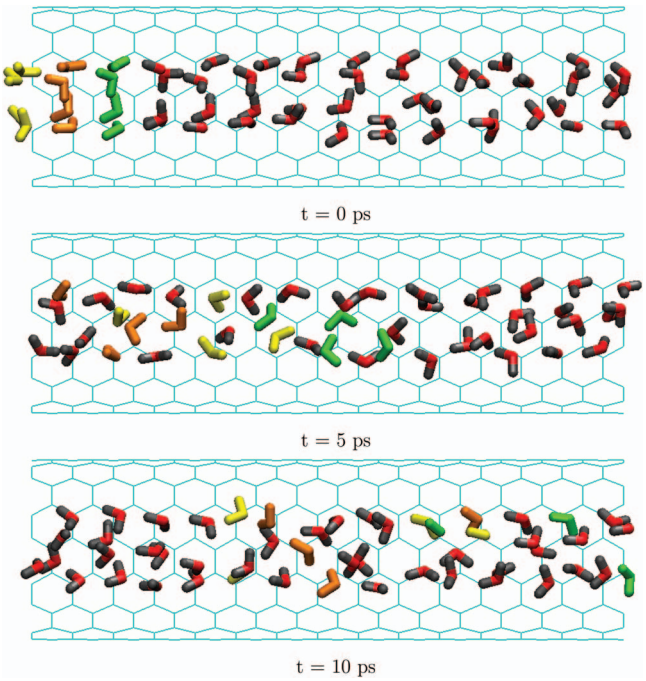

FIG. 6. An illustration of the "diffusive" conduction mode for TIP3P in the (8,8) nanotube. Carbon atoms are cyan, oxygen atoms are red, and hydrogen atoms are gray, except for three square ring configurations highlighted in yellow, orange, and green. We note that the highlighted ring structures present at $t = 0$ break up completely as the water molecules pass through the nanotube. Note that part of carbon nanotube is not displayed for clarity.

conduction modes can and do occur to some extent for all three models, but the slower cluster-by-cluster mode is favored by TIP4P/2005 and SPC/E, and the faster diffusive mode by TIP3P. In the (8,8) case, SPC/E has a higher flow rate than TIP4P/2005, likely due to the higher fraction of ring-free molecules found for that model (Table III). For the (9,9) nanotube, SPC/E and TIP4P/2005 have the same fraction of ring-free molecules, and similar flow rates.

It is perhaps worth pointing out that density differences alone cannot account for the observed differences in flow rate. This is most apparent in the (9,9) case [Fig. 4 (bottom panel)], where the most probable nanotube densities are similar for TIP3P and TIP4P/2005, which have very different flow rates, and significantly different for TIP4P/2005 and SPC/E, which have similar flow rates.

IV. SUMMARY AND CONCLUSION

We have used molecular dynamics simulations to investigate pressure-driven water transport through (8,8) and (9,9) CNTs. Three different water models, TIP3P, SPC/E, and TIP4P/2005, were considered and the flow rates even under relatively high pressure were strikingly different, with the fastest (TIP3P) being about five times faster than the slowest (TIP4P/2005) in both nanotubes. We trace the different flow rates to different degrees of structure of the water in the nanotube channels. The TIP4P/2005 model tends to form stacked ring structures, giving rise to a "cluster-by-cluster" flow mode with many planar ring clusters moving as single units through the nanotube. To a lesser extent, this is also true of SPC/E. This mode of conduction is slower than that observed for TIP3P, where ring structures occur less frequently, and tend to break apart as water flows through the channel. This results in a faster "diffusive" conduction mode where the molecules move as separate particles, rather than as parts of larger clusters.

We note again that our results apply to CNTs that are sufficiently wide for the confined water molecules to form various ring structures. We would not expect such severe model dependence for narrow CNTs where water molecules form only hydrogen-bonded chains, and single-files conduction is observed.[10–17]

It is not possible to determine which water model is most consistent with the behavior of real water in CNTs, but we do note that TIP4P/2005 is widely regarded as among the best water models available for bulk properties. To the best of our knowledge, the TIP4P/2005 model has not been previously used in studies of water flow through CNTs. It is also important to emphasize that model differences, which might not have a large influence on the properties of bulk water, can have large effects on the structure and flow of confined water.

ACKNOWLEDGMENTS

The financial support of the Natural Science and Engineering Research Council of Canada is gratefully acknowledged. This research has been enabled by the use of WestGrid and Compute/Calcul Canada computing resources, which are funded in part by the Canada Foundation for Innovation, Alberta Innovation and Science, BC Advanced Education, and the participating research institutions. WestGrid and Compute/Calcul Canada equipment is provided by IBM, Hewlett Packard and SGI.

[1] A. Alexiadis and S. Kassinus, Chem. Rev. **108**, 5014 (2008).
[2] J. C. Rasaiah, S. Garde, and G. Hummer, Annu. Rev. Phys. Chem. **59**, 713 (2008).
[3] J. K. Holt, Adv. Mater. **21**, 3542 (2009).
[4] J. K. Holt, H. G. Park, Y. Wang, M. Stadermann, A. B. Artyukhin, C. P. Grigoropoulos, A. Noy, and O. Bakajin, Science **312**, 1034 (2006).
[5] M. Whitby, L. Cagnon, M. Thanou, and N. Quirke, Nano Lett. **8**, 2632 (2008).
[6] X. Qin, Q. Yuan, Y. Zhao, S. Xie, and Z. Liu, Nano Lett. **11**, 2173 (2011).
[7] C. Y. Won, S. Joseph, and N. R. Aluru, J. Chem. Phys. **125**, 114701 (2006).
[8] S. Joseph and N. R. Aluru, Nano Lett. **8**, 452 (2008).
[9] T. A. Pascal, W. A. Goddard, and Y. Jung, Proc. Natl. Acad. Sci. U. S. A. **108**, 11794 (2011).
[10] G. Hummer, J. C. Rasaiah, and J. P. Noworyta, Nature **414**, 188 (2001).
[11] A. Waghe, J. C. Rasaiah, and G. Hummer, J. Chem. Phys. **117**, 10789 (2002).
[12] A. Berezhkovskii and G. Hummer, Phys Rev. Lett. **89**, 064503 (2002).
[13] A. Kalra, S. Garde, and G. Hummer, Proc. Natl. Acad. Sci. U. S. A. **100**, 10175 (2003).
[14] A. Kalra, G. Hummer, and S. Garde, J. Phys. Chem. B **108**, 544 (2004).
[15] K. Wu, B. Zhou, P. Xiu, W. Qi, R. Wan, and H. Fang, J. Chem. Phys. **133**, 204702 (2010).
[16] A. Waghe, J. C. Rasaiah, and G. Hummer, J. Chem. Phys. **137**, 044709 (2012).
[17] T. B. Sisan and S. Lichter, Phys. Rev. Lett. **112**, 044501 (2014).
[18] B. Corry, J. Phys. Chem. B **112**, 1427 (2008).
[19] B. Corry, Energy Environ. Sci. **4**, 751 (2011).
[20] J. S. Babu and S. P. Sathian, J. Chem. Phys. **134**, 194509 (2011).
[21] Y. Xue and M. Chen, Nanotechnology **17**, 5216 (2006).
[22] J. Goldsmith and C. C. Martens, J. Phys. Chem. Lett. **1**, 528 (2010).
[23] H. Kumar, B. Mukherjee, S.-T. Lin, C. Dasgupta, A. K. Sood, and P. K. Maiti, J. Chem Phys. **134**, 124105 (2011).

[24]L. Wang, R. S. Dumont, and J. M. Dickson, J. Chem. Phys. **138**, 124701 (2013).
[25]W. D. Nicholls, M. K. Borg, D. A. Lockerby, and J. M. Reese, Mol. Simul. **38**, 781 (2012).
[26]J. A. Thomas and A. J. H. McGaughey, J. Chem. Phys. **128**, 084715 (2008).
[27]J. A. Thomas and A. J. H. McGaughey, Nano Lett. **8**, 2788 (2008).
[28]J. A. Thomas and A. J. H. McGaughey, Phys. Rev. Lett. **102**, 184502 (2009).
[29]K. Falk, F. Sedlmeire, L. Joly, R. R. Netz, and L. Bocquet, Nano. Lett. **10**, 4067 (2010).
[30]W. L. Jorgensen, J. Chandrasekhar, J. D. Madura, R. W. Impey, and M. L. Klein, J. Chem. Phys. **79**, 926 (1983).
[31]H. J. C. Berendsen, J. R. Grigera, and T. P. Straatsma, J. Phys. Chem. **91**, 6269 (1987).
[32]M. W. Mahoney and W. L. Jorgensen, J. Chem. Phys. **112**, 8910 (2000).
[33]Y. Nakamura and T. Ohno, Mater. Chem. Phys. **132**, 682 (2012).
[34]S. W. Rick, J. Chem. Phys. **120**, 6085 (2004).
[35]A. Alexiadis and S. Kassinos, Chem. Eng. Sci. **63**, 2793 (2008).
[36]A. Alexiadis and S. Kassinos, Mol. Simul. **34**, 671 (2008).
[37]B. A. Bauer, S. Ou, S. Patel, and K. Siva, Phys. Rev. E **85**, 051506 (2012).
[38]J. L. F. Abascal and C. Vega, J. Chem. Phys. **123**, 234505 (2005).
[39]C. Vega and J. L. F. Abascal, Phys. Chem. Chem. Phys. **13**, 19663 (2011).
[40]Y. Duan, C. Wu, S. Chowdhury, M. C. Lee, G. Xiong, W. Zhang, R. Yang, P. Cieplak, R. Luo, T. Lee, J. Caldwell, J. Wang, and P. Kollman, J. Comput. Chem. **24**, 1999 (2003).
[41]D. van der Spoel, E. Lindahl, B. Hess, G. Groenhof, A. E. Mark, and H. J. C. Berendsen, J. Comput. Chem. **26**, 1701 (2005).
[42]T. Darden, D. York, and L. Pedersen, J. Chem. Phys. **98**, 10089 (1993).
[43]G. Bussi, D. Donadio, and M. Parrinello, J. Chem. Phys. **126**, 014101 (2007).
[44]F. Zhu, E. Tajkhorshid, and K. Schulten, Biophys. J. **86**, 50 (2004).
[45]K. Koga, R. D. Parra, H. Tanaka, and X. C. Zeng, J. Chem. Phys. **113**, 5037 (2000).
[46]A. Luzar and D. Chandler, J. Chem. Phys. **98**, 8160 (1993).